

Fixation times in differentiation and evolution in the presence of bottlenecks, deserts, and oases

Tom Chou^{1,2,*}, Yu Wang³

¹*Dept. of Biomathematics, UCLA, Los Angeles, CA 90095-1766, USA*

²*Dept. of Mathematics, UCLA, Los Angeles, CA 90095-1555, USA*

³*Institute for Information and System Sciences, Xi'an Jiaotong University, Xi'an, China*

Abstract

Cellular differentiation and evolution are stochastic processes that can involve multiple types (or states) of particles moving on a complex, high-dimensional state-space or “fitness” landscape. Cells of each specific type can thus be quantified by their population at a corresponding node within a network of states. Their dynamics across the state-space network involve genotypic or phenotypic transitions that can occur upon cell division, such as during symmetric or asymmetric cell differentiation, or upon spontaneous mutation. Waiting times between transitions can be nonexponentially distributed and reflect *e.g.*, the cell cycle. Here, we use a multi-type branching processes to study first passage time statistics for a single cell to appear in a specific state. We present results for a sequential evolutionary process in which L successive transitions propel a population from a “wild-type” state to a given “terminally differentiated,” “resistant,” or “cancerous” state. Analytic and numeric results are also found for first passage times across an evolutionary chain containing a node with increased death or proliferation rate, representing a desert/bottleneck or an oasis. Processes involving cell proliferation are shown to be “nonlinear” (even though mean-field equations for the expected particle numbers are linear) resulting in first passage time statistics that depend on the position of the bottleneck or oasis. Our results highlight the sensitivity of stochastic measures to cell division fate and quantify the limitations of using certain approximations and assumptions (such as fixed-population and mean-field assumptions) in evaluating fixation times.

Keywords: Stochastic evolution, Bellman-Harris branching process, bottleneck, oasis, fixation times

1. Introduction

Stochastic models of populations have long been applied to biological processes such as stem cell dynamics [1, 2], tumorigenesis [3, 4, 5, 6, 7, 8], cellular aging [9], and organismal evolution [10, 11]. In such applications, one is often interested in the statistics of the time it takes for members of a population to first arrive at a specific “absorbing” state. Such a state may represent, for example, a high fitness phenotype that eventually takes over the entire population.

A classic biomedical application of first passage times of a single conserved entity arises in models of cancer progression that attempt to describe the survival probability of patients as a function of time after initial diagnosis or treatment. In the Knudsen hypothesis of cancer progression (illustrated in Fig. 1) [12, 13], an individual acquires a certain number of sequential mutations or “hits” before acquiring cancer [14, 15, 5]. If multiple rare transitions are required before onset of disease, we can define the probability of transition from state ℓ to state $\ell + 1$ in time dt as $w_\ell(t)dt$. The overall waiting-time distribution to first arrive at

*Corresponding author

Email address: tomchou@ucla.edu (Tom Chou^{1,2})

¹Tel: 310-206-2787, Fax: 310-825-8685

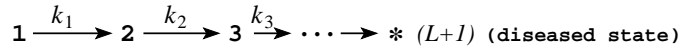


Figure 1: Multistage model in disease progression. When multiple steps are before the system reaches diseased state $L + 1$, an L -fold convolution of the state-dependent individual waiting time distributions provides the overall waiting time distribution and the survival probability against disease.

the diseased state $\ell = L + 1$ is a convolution of all the $w_\ell(t)$ and can be easily expressed using Laplace transforms: $\tilde{W}(s) = \prod_{\ell=1}^L \tilde{w}_\ell(s)$. Since each mutation is considered rare, the event times of each mutation are exponentially distributed. If all transitions occur at the same rate, $k_0 = k_1 = \dots = k$, $w_\ell(t) = ke^{-kt}$, and $\tilde{W}(s) = k^L/(s+k)^L$. The inverse Laplace transform then gives [16]

$$W(t)dt = k \frac{(kt)^{L-1} e^{-kt}}{(L-1)!} dt. \quad (1)$$

This expression assumes that all the transition rates are equally rate-limiting. If $kt \ll 1$, the survival probability against disease onset is approximately

$$S(t) = 1 - \int_0^t W(t') dt' = \frac{\Gamma(L, kt)}{(L-1)!} \approx 1 - \frac{(kt)^L}{L!}, \quad (2)$$

If sufficiently accurate fitting of this expression to measured $S(t)$ can be performed, the number of mutations, or “hits” L before onset of cancer can be inferred. Using this Knudsen hypothesis [14], typical cancers have yielded $L \sim 4 - 15$ or higher [17, 18].

Such studies implicitly assume a “single-particle” picture of a conserved random walker that eventually reaches a target. On a cellular level this picture is appropriate for a single immortal and nonproliferating cell that successively acquires different mutations. Estimates and scaling relationships of first passage times of conserved particles on complex networks have been developed in more general contexts [19, 20]. Analogous results have been developed for a fixed multiple number of noninteracting particles [21]. Inverse problems (similar to the inference of the number of mutations in Knudsen’s hypothesis) have also been recently explored. Li, Kolomeisky, and Valleriani [22] considered how first passage times of a conserved random walker can be used to estimate the shortest paths to the absorbing site, even for nonexponentially distributed waiting times between jumps within the network. First passage times of Brownian motion and random walks have also been used to infer properties of continuous energy landscapes [23, 24].

If a network is finite, and all nodes are connected, conserved particles will always arrive at an absorbing state and the survival probability $S(t \rightarrow \infty) \rightarrow 0$. However, in the presence of other pathways for particle annihilation, the absorbing site may never be reached. Additional particles need to be continuously injected into the network in order for one of them to eventually arrive, with certainty, at a specific absorbing state [25]. Alternative annihilation pathways and immigration lift the fixed population constraint and is an essential feature in cell and population biology.

Canonical Wright-Fisher and Moran models of evolution consider a population of organisms distributed between two states [10]. Evolution across multiple states or fitness levels have also been explored in models of stochastic tunneling [26, 27, 28]. Many of these models impose a fixed mean populations and do not resolve the possible microscopic transitions an organism can take during the evolution process. These differences in the “microscopic” mechanisms of evolution are especially distinguishable in cell biology, in which changes in genotype or phenotype can arise spontaneously in an individual cell, or from symmetric or asymmetric replication. Different cell fates are clearly important in the context of stem cell differentiation and cancer [11, 8, 2, 29]. Moreover, due to cell death, cell populations can have high turnover within the timescale of their evolution. Therefore, the total instantaneous population need not be fixed, even if the ensemble-averaged population remains constant. We shall see that the different transitions inherent in cellular differentiation and evolution, as well as fluctuations in population, can qualitatively affect fixation times.

We begin by considering a whole population of cells or “particles” in a network. Fixation in this context will be defined by a single cell or particle first arriving at an absorbing node. Absorbing nodes can represent,

for example, terminally differentiated, fully drug-resistant, or highly fit, fully cancerous states. We first treat only a noninteracting population and temporarily neglect any regulation or population constraint such as carrying capacity. The analysis is simplified when the total population is unconstrained; however, we will extend mathematical framework in order to resolve the effects of different types of allowed transitions. To describe the evolution of a whole population of cells and their arrival times to the absorbing nodes, we exploit a multi-type Bellman-Harris branching process that allows for general distributions of waiting times between transition events [30, 10, 31]. Our approach is related the analysis of Portier, Sherman, and Kopp-Schneider [4] and the simulations of Sherman and Portier [3], but we provide numerical, asymptotic, and exact mean-field results to illustrate the effects of order-dependent transition rates. New approximations for analyzing processes constrained by carrying capacity are also developed.

In the next section, for completeness, we present the continuous-time semi-Markov multi-type branching formalism and derive the equations obeyed by the probability generating functions for particle numbers at each node in the network. The corresponding equations for the survival probabilities are then derived. By further assuming exponentially distributed waiting times and a sequential evolution model, we explicitly derive the matrix Riccati equation governing the evolution of survival probabilities in the presence of immigration. In the Results, we present analytic, asymptotic, and numerical results for survival probabilities and mean first passage times. Effects of the probabilities of the different cellular transitions on our results are explored. A breakdown of mean-field theories of survival probabilities (even when particles are noninteracting) is described. Effects of heterogeneity in the transition rates are discussed in the context of evolutionary oases and bottlenecks. The conditions under which the order of the transition rates along the evolutionary chain can affect the survival probabilities and first passage times are investigated. Finally, we summarize our results, discuss related biological applications, and describe extensions and future directions.

2. Mathematical Model

Here, we describe in detail a stochastic multi-type population in the presence of immigration. The general framework is presented before restricting ourselves to exponentially distributed inter-transition times and sequential evolution for a more detailed analysis.

2.1. Multi-type Branching Process

Our analysis of the problem is most efficiently performed using an age-dependent multi-type branching process where a parent cell of type k waits a time τ before dividing into a number of cells of possibly different types. Cells with different numbers of mutations, or at different stages of differentiation, can have different distributions of waiting times before proliferation. Moreover, each cell type, upon proliferation, can yield different numbers of new cells. In the analysis of this multi-type branching process, we employ the probability generating function (pgf)

$$F_k(\mathbf{z}; t) = \sum_{n_1=0}^{\infty} \cdots \sum_{n_{L+1}=0}^{\infty} P_k(\mathbf{n}; t) z_1^{n_1} \cdots z_{L+1}^{n_{L+1}}, \quad (3)$$

in which $\mathbf{z} = (z_1, z_2, \dots, z_L, z_{L+1})$ and $\mathbf{n} = (n_1, n_2, \dots, n_L, n_{L+1})$. $P_k(\mathbf{n}; t)$ is the probability at time t the entire population contains n_j cells of type j , given that the system started at $t = 0$ with a single cell of type k . We assume that all daughter cells proliferate independently and that each branching event of a single cell of type k yields m_1, m_2, \dots, m_{L+1} cells of type $1, 2, \dots, L + 1$ with probability $a^{(k)}(m_1, m_2, \dots, m_{L+1}) \equiv a^{(k)}(\mathbf{m})$.

What equation of evolution does $F_k(\mathbf{z}; t)$ obey? For notational simplicity, it is easiest to first consider a single-species branching process described by the simple pgf $F(z, t)$ that corresponds to $P(n, t|1, 0)$, the probability of n particles at time t , given a single parent particle at $t = 0$. If we now define $F(z, t|\tau)$ as

the generating function of the process conditioned on the original parent particle having first “branched” between τ and $\tau + d\tau$, we write the recursion

$$F(z, t|\tau) = \begin{cases} z, & t < \tau \\ A[F(z, t - \tau)], & t \geq \tau, \end{cases} \quad (4)$$

where

$$A[z] = \sum_{m=0}^{\infty} a(m)z^m \quad (5)$$

defines the probability $a(m)$ that a particle splits into m identical particles upon branching. We now average Eq. (4) over the distribution of waiting times between branching events, $g(\tau)$, to find

$$\begin{aligned} F(z, t) &\equiv \int_0^{\infty} F(z, t|\tau)g(\tau)d\tau \\ &= z \int_t^{\infty} g(\tau)d\tau + \int_0^t A[F(z, t - \tau)]g(\tau)d\tau. \end{aligned} \quad (6)$$

This Bellman-Harris branching process [30, 31] is defined by two parameter functions, $a(m)$, the vector of progeny number probabilities, and $g(\tau)$, the probability density function (pdf) for waiting times between branching events for each particle. Given a single-particle initial condition, $F(z, 0) = z$ and Eq. 6 can be solved to find a $F(z, t)$, from which $P(n, t|1, 0)$ can be generated.

For our multi-state model, we simply generalize Eq. 6 to a multi-type process, where particles at different states constitute different types. The vector of progeny probabilities $a(m)$ now becomes a matrix $a^{(k)}(\mathbf{m})$ coupling the birth of different types of particles from a parent particle of state k . Thus,

$$A_k[\mathbf{z}] \equiv \sum_{m_1=0}^{\infty} \cdots \sum_{m_{L+1}=0}^{\infty} a^{(k)}(\mathbf{m})z_1^{m_1} \cdots z_{L+1}^{m_{L+1}} \quad (7)$$

is the pgf of the progeny number distribution matrix associated with each branching event. The relationship for the multi-type pgf becomes

$$F_k(\mathbf{z}; t) = z_k \int_t^{\infty} g_k(\tau)d\tau + \int_0^t A_k[\mathbf{F}(\mathbf{z}; t - \tau)]g_k(\tau)d\tau, \quad (8)$$

where $g_k(\tau)d\tau$ is the probability that a particle of type k branches between time τ and $\tau + d\tau$ after it was created.

Consider $S_k(t) = F_k(z_{j \neq L+1} = 1, z_{L+1} \rightarrow 0^+; t)$, the probability of not having formed a cell of type $L + 1$ up to time t given one initial parent cell in node k at time $t = 0$. Setting $z_{j \neq L+1} = 1$ in Eq. 8, we find

$$S_{j \neq L+1}(t) = \int_t^{\infty} g_j(\tau)d\tau + \int_0^t A_j[\mathbf{S}(t - \tau)]g_j(\tau)d\tau, \quad (9)$$

where $\mathbf{S} = \{S_{j \neq L+1}\}$ is the vector of survival probabilities initiated by a single cell in state j . Since $L + 1$ is defined as an absorbing state, we are interested in the first time a particle first arrives at node $L + 1$. Therefore, by setting $A_{L+1} = 0$, we allow particles to only accumulate in state $L + 1$, and define the survival probability $S_{L+1}(t) = F_{L+1}(z_{i \neq L+1} = 1, z_{L+1} = 0) = 0$. This “boundary condition” in the starting positions, along with the initial conditions $S_{j \neq L+1}(t = 0)$, completely defines the problem for $\mathbf{S}(t)$.

Note that our model neglects particle-particle interactions and that the transition probabilities $a^{(k)}(\mathbf{m})$ do not depend on the number of particles in the network. Therefore, all initial particles behave independently and the survival probability associated with a system initiated with N cells at node $i = 1$ is simply $\Sigma(t) \equiv [S_1(t)]^N$. Provided that no particles leave the network other than through state $L + 1$, $S_k(t \rightarrow 0) = o(t^{-1})$,

the *mean* first arrival time $T = \int_0^\infty \Sigma(t) dt$ is well-defined. However, if the particle dynamics include death, there can be extinction before node $L + 1$ is reached, and the mean arrival time T will diverge. In this case, a more useful measure of the speed of evolution would be the mean arrival time conditioned on arrival at $L + 1$ [25].

A process that ensures arrival to the final state $L + 1$ is injection of particles from an external source. We can extend the branching process formulation to include immigration of parent particles into the system [32, 33]. Suppose that particles of type i are injected into the system with inter-injection times distributed according to $h_i(\tau)$. Upon assuming an initially *empty* network, the pgf for the total particle numbers resulting from independently injecting type i particles is thus [32, 33]

$$\Phi_i(\mathbf{z}; t) = \int_t^\infty h_i(\tau) d\tau + \int_0^t \Phi_i(\mathbf{z}; t - \tau) B_i[F_i(\mathbf{z}; t - \tau)] h_i(\tau) d\tau, \quad (10)$$

where $B_i[z_i] = \sum_{n_i=0}^\infty b_i(n_i) z_i^{n_i}$ is the pgf constructed from the probability $b_i(n_i)$ that n_i particles are simultaneously injected into state i during each immigration event. For example, if particles are injected only three-at-a-time into node i , $b_i(n_i) = \delta_{n_i,3}$. In the cellular biology setting, immigration into the i^{th} state can arise from spontaneous mutation or from mutations acquired during replication of an “external” (not included in the states k) wild-type cell. Therefore, $B_i[F_i] = b_i(1)F_i + b_i(2)F_i^2$, where $b_i(1)$ and $b_i(2)$ are the probabilities that during each event, one and two cells immigrate into state i , respectively. Since these are the only allowed mechanisms of cellular immigration, $b_i(1) + b_i(2) = 1$. In the presence of immigration into all possible stages, the pgf of the total particle number is thus $\Psi(\mathbf{z}; t) = \prod_{i=1}^L \Phi_i(\mathbf{z}; t)$.

Upon using Eqs. 8 and 10 to find $\Psi(\mathbf{z}; t)$, one can construct quantities such as the expected number of cells of type k , $\langle n_k(t) \rangle = (\partial \Psi(\mathbf{z}; t) / \partial z_k) |_{\mathbf{z}=1}$, and the probability that no cells have yet reached the fully mutated state $i = L + 1$: $\Sigma(t) = \Psi(z_{j \leq L} = 1, z_{L+1} \rightarrow 0; t)$. Without loss of generality, we henceforth restrict our analysis to immigration only into node $i = 1$. This limit can be explicitly constructed by letting the times between consecutive immigration into stages $i > 1$ diverge. For example, if $h_{i \neq 1}(\tau) = \lim_{T_i \rightarrow \infty} \delta(\tau - T_i)$, Eq. 10 then yields $\Phi_{i \neq 1} \rightarrow 1$ and $\Psi(\mathbf{z}; t) = \Phi_1(\mathbf{z}; t)$.

When $i = 1$, Eq. 10 shows that the overall survival probability $\Sigma(t)$ in the presence of cell immigration obeys

$$\Sigma(t) = \int_t^\infty h_1(\tau) d\tau + \int_0^t \Sigma(t - \tau) B_1[S_1(t - \tau)] h_1(\tau) d\tau, \quad (11)$$

By solving Eqs. 9 for $S_1(t)$ and using the result in Eq. 11, we can find the overall survival probability of an initially empty network after cells begin to immigrate into state $i = 1$. Since cells are not conserved (in particular, they can die), $S_{j \neq L+1}(t \rightarrow \infty)$ need not vanish. However, provided particle injection into state $i = 1$ persists, the absorbing state will eventually be reached with certainty and $\Sigma(t \rightarrow \infty) \rightarrow 0$. Depending on the immigration frequency and number of imported particles per injection event, reaching the terminal state may be rate-limited by either the internal dynamics defined by $a^{(k)}(\mathbf{m})$ and $g(\tau)$, or by immigration described by $b_i(n_i)$ and $h_i(\tau)$. Finally, the *mean* first passage time (MFPT) can be calculated from [25, 34]

$$T = \int_0^\infty \Sigma(t) dt. \quad (12)$$

2.2. Exponentially distributed sequential processes

Our results can be simplified if branching and immigration times are exponentially distributed, $g_j(\tau) = \lambda_j e^{-\lambda_j \tau}$ and $h_1(\tau) = \beta_1 e^{-\beta_1 \tau}$. After some algebra, Eqs. 9 and 11 become

$$\frac{dS_k(t)}{dt} = \lambda_k A_k[\mathbf{S}(t)] - \lambda_k S_k(t), \quad (13)$$

$$\frac{d\Sigma(t)}{dt} = -\beta_1 (1 - B_1[S_1(t)]) \Sigma(t). \quad (14)$$

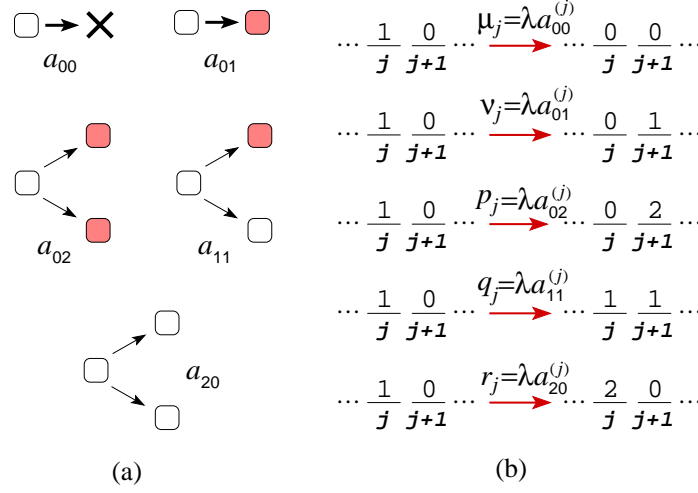


Figure 2: (a) The five possible transitions of a single cell at an initial stage (white) and their probabilities a_{mn} . Dividing cells can produce daughters at a more differentiated or mutated stage (red). Since these are the only possible steps, $a_{00} + a_{01} + a_{11} + a_{20} + a_{02} = 1$. Note that in general time between transitions can be age-dependent and do not have to be exponentially distributed in time. (b) When inter-transition times are exponentially distributed, the rates of each process can be defined in terms of the branching rate and the branching probabilities $a_{mn}^{(k)}$ at each node k .

Thus, the survival probability can be explicitly expressed as

$$\Sigma(t) = \exp \left[-\beta_1 \int_0^t (1 - B_1[S_1(t')]) dt' \right], \quad (15)$$

where $S_1(t)$ is found from solving Eq. 13.

The analysis can be further simplified by assuming a sequential evolution processes where each division by a cell can yield only daughter cells of the same type or of an incrementally more differentiated (or mutated) type. In other words, when a type k cell attempts to proliferate, either death occurs, or daughters of only type k and/or $k+1$ are produced. Consequently, $a^{(k)}(\mathbf{m}) = 0$ for any $m_j > 0$ when $j \neq k, k+1$. Therefore, F_{k+1} in Eq. 8 is coupled to F_k through the integrand $A_k[F_1, F_2, \dots, F_{L+1}]$, and one must solve for all F_j . To be explicit, if the only possible transitions are those depicted in Fig. 2(a), we find

$$A_k[\mathbf{z}] = a_{00}^{(k)} + a_{01}^{(k)} z_{k+1} + a_{11}^{(k)} z_k z_{k+1} + a_{20}^{(k)} z_k^2 + a_{02}^{(k)} z_{k+1}^2. \quad (16)$$

In the context of cell biology, the probabilities $a_{00}, a_{01}, a_{02}, a_{11}$ and a_{20} shown in Fig. 2 represent death, somatic mutation, symmetric differentiation, asymmetric differentiation, and replication after each attempt at cell division. For $g_j(\tau) = \lambda_j e^{-\lambda_j \tau}$ the individual rates of these processes are given by $\mu_k = \lambda_k a_{00}^{(k)}$, $\nu_k \equiv \lambda_k a_{01}^{(k)}$, $r_k \equiv \lambda_k a_{20}^{(k)}$, $q_k \equiv \lambda_k a_{11}^{(k)}$, and $p_k = \lambda_k a_{02}^{(k)}$, and shown in Fig. 2(b). Similarly, we define $\alpha_1 = \beta_1 b_1(1)$ and $\alpha_2 = \beta_1 b_1(2)$ as the rates of injecting a single particle and double particle into state $i = 1$, respectively. The values μ_k, ν_k, p_k, q_k , and r_k correspond to *rates* of death, somatic mutation, symmetric differentiation, asymmetric differentiation, and symmetric replication, respectively, of cells in state k .

A sequential evolution model can thus be constructed by assigning a set of transition probabilities at each successive cell state, or node, as shown in Fig. 3. Eq. 13 for $S_k(t)$ and the associated initial condition thus reduces to

$$\frac{dS_k(t)}{dt} = \mu_k + \nu_k S_{k+1} + r_k S_k^2 + q_k S_k S_{k+1} + p_k S_{k+1}^2 - \lambda_k S_k \quad (17)$$

and $S_{k \leq L}(0) = 1$, $S_{L+1}(t) = 0$.

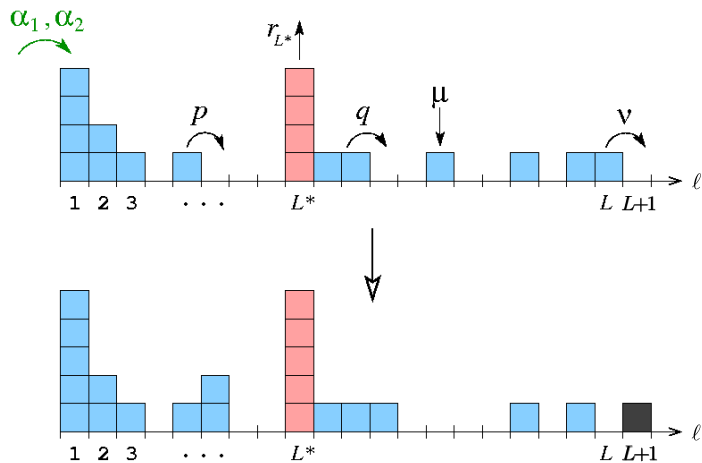


Figure 3: A sequential evolution model. The possible transitions are labeled. Heterogeneities in the transition rates along the sequence can be easily incorporated in our computation. Localized heterogeneities (*e.g.*, at site L^*) can be used to model oases or bottlenecks. Our analysis focusses on the first arrival time to state $L + 1$.

3. Results

In this section, we present both analytic and numeric results for $S_k(t)$, $\Sigma(t)$, and the MFPTs T for sequential, exponentially distributed processes described by Figs. 2 and 3. We discuss their properties as functions of transition rates and system size, and compare these results with those obtained from the simplest mean-field approximations.

3.1. Linear processes

For “linear” dynamics, defined by $p_k = q_k = r_k = 0$, Eqs. 17 are linear and can be solved exactly using Laplace transforms:

$$\tilde{S}_k(s) = \frac{1}{s} \left[1 - \prod_{i=k}^L \frac{\nu_i}{(s + \lambda_i)} \right]. \quad (18)$$

This result explicitly shows that $\tilde{S}_1(s)$, and hence $\Sigma(t)$ is invariant with respect to the order of $\mu_i + \nu_i = \lambda_i$. Therefore, heterogeneity in the transition rates of this linear Poisson process does not influence the first passage times to the absorbing state. Similarly, the survival probability for a sequential process with general waiting time distribution $g_k(\tau)$ can be found from solving Eq. 9 to find $\tilde{S}_1(s) = s^{-1} [1 - \prod_{i=1}^L a_{01}^{(i)} \tilde{g}_i(s)]$, which is also clearly independent of the order of the transitions.

Eq. 18 can be inverted to obtain explicit expressions for $S_k(t)$. $S_1(t)$ can be then used in Eq. 15 to obtain the full survival probability $\Sigma(t)$, and ultimately the MFPT using Eq. 12. For uniform $\lambda_k = \lambda$, Eq. 18 simplifies to

$$S_k(t) = 1 - \left(\frac{\nu}{\lambda} \right)^{L-k+1} \left[1 - \frac{\Gamma(L-k+1, \lambda t)}{\Gamma(L-k+1)} \right], \quad (19)$$

which is equivalent to the survival probability of a zero-range process with death [35].

If there is no immigration nor death ($\mu = 0$ and $\lambda = \nu$), the process is analogous to an irreversible multi-step Moran process in which a parent cell immediately dies after producing one mutated/evolved/differentiated daughter cell. The conservation of particles means that eventual arrival to any connected node $L + 1$ is certain. For an initial condition of N particles in node $k = 1$, the mean time for a first cell to arrive at the terminal state $L + 1$ is

$$\begin{aligned}
T &= \nu^{-1} \int_0^\infty \left(\frac{\Gamma(L, y)}{\Gamma(L)} \right)^N dy \\
&\sim \frac{1}{\nu} \left[\frac{(L-1)\Gamma(L)}{N-1} \right]^{1/L}, \quad \frac{1}{L} \left[\frac{(L-1)\Gamma(L)}{N-1} \right]^{1/L} \ll 1.
\end{aligned} \tag{20}$$

If there is death ($\mu > 0$) but also immigration (α_1 and/or $\alpha_2 > 0$), the explicit expression for the overall survival probability $\Sigma(t)$ can be found by using Eq. 18 in Eq. 15. In the constant $\lambda = \mu + \nu$ case, we find

$$\begin{aligned}
\Sigma(t) &= \exp \left[-\alpha_1 \int_0^t (1 - S_1(t')) dt' \right] \exp \left[-\alpha_2 \int_0^t (1 - S_1^2(t')) dt' \right] \\
&= \exp \left[-\frac{(\alpha_1 + 2\alpha_2)}{\lambda} \left(\frac{\nu}{\lambda} \right)^L \left(\lambda t - L - \lambda t \frac{\Gamma(L, \lambda t)}{\Gamma(L)} + \frac{\Gamma(L+1, \lambda t)}{\Gamma(L)} \right) \right] \\
&\quad \times \exp \left[-2 \frac{\alpha_2}{\lambda} \left(\frac{\nu}{\lambda} \right)^{2L} \left(L + \lambda t \frac{\Gamma(L, \lambda t)}{\Gamma(L)} - \frac{\Gamma(L+1, \lambda t)}{\Gamma(L)} - \frac{\lambda t}{2} \right) \right] \exp \left[\alpha_2 \left(\frac{\nu}{\lambda} \right)^{2L} \int_0^t \left(\frac{\Gamma(L, \lambda t')}{\Gamma(L)} \right)^2 dt' \right].
\end{aligned} \tag{21}$$

When $\alpha_2 = 0$ (no double-particle immigration), the integral $T = \int_0^\infty \Sigma(t) dt$ can be approximated in the small and large limits of $\Omega \equiv (\alpha_1/\lambda)(\nu/\lambda)^L$ by considering the structure of integrand $\Sigma(t)$ in Eq. 12[36]:

$$T \approx \begin{cases} \frac{L}{\lambda} \left[1 + \frac{1}{\Omega L} \right], & \Omega \equiv \frac{\alpha_1}{\lambda} \left(\frac{\nu}{\lambda} \right)^L \ll 1 \\ \frac{1}{\lambda} \Gamma \left(\frac{L+2}{L+1} \right) \left[\frac{(L+1)!}{\Omega L} \right]^{\frac{1}{L+1}}, & \frac{\Omega}{L!} \gg 1. \end{cases} \tag{22}$$

Fig. 4(a) shows exact survival probabilities of the homogeneous sequential linear process for different values of chain length L . For comparison, we plot curves corresponding to different rate parameters μ and ν relative to the total uniform transition rate $\lambda = \mu + \nu$. Fig. 4(b) plots $\ln \lambda T$ as a function of chain length L .

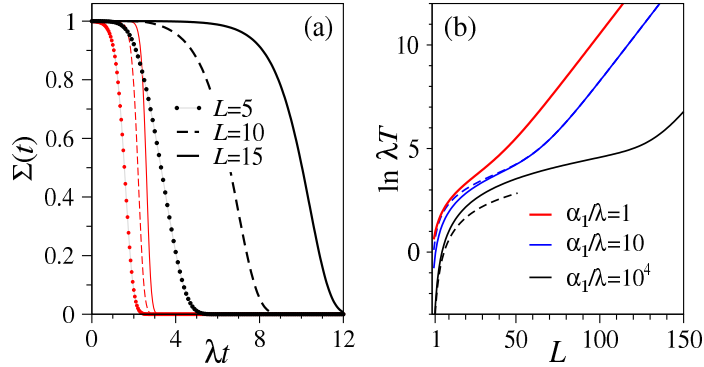


Figure 4: (a) Survival probabilities for $L = 5, 10, 15$ plotted as a function of λt . The set of three thin red curves decaying at short times correspond to $\alpha_1 = \lambda, \alpha_2 = 0, \mu/\lambda = 0.01, \nu/\lambda = 0.99$, while the three black curves decaying at longer times correspond to $\mu/\lambda = \nu/\lambda = 0.5$. The effects of increased chain length L are more dramatic when particle decay is faster and length-dependent stochastic tunneling becomes rate-limiting. (b) Plots of $\ln(\lambda T)$ as a function of L for $\alpha_1/\lambda = 1, 10, 10^4$ with fixed $\alpha_2 = 0, \mu/\lambda = 0.1$, and $\nu/\lambda = 0.9$. The two dashed curves correspond to the asymptotic limits in Eq. 22.

For large ΩL , the rate limiting step is immigration and the MFPT is approximately the inter-immigration time, normalized by the probability each immigration event eventually leads to fixation (the $\Omega \ll 1$ limit in Eq. 22).

3.2. Nonlinear processes

Now, consider cell replication processes where $p_k + q_k + r_k > 0$. When these higher order cellular processes arise, Eq. 17 is nonlinear for $N > 1$, and the evaluation of survival probabilities and first passage times must be approximated or computed numerically. From Eq. 15, we can see that for sufficiently small α_1/λ , the survival probability will scale as $\Sigma(t) \sim e^{-\alpha_1(1-\bar{S}_1)t}$. Note that if $\mu_k = 0$ for all k , the only steady-state solution to Eq. 17 is $S_k(t \rightarrow \infty) \equiv \bar{S}_k = 0$. Hence, $\Sigma(t) \sim e^{-\alpha_1 t}$, indicating that immigration is the rate limiting step. In the following we will provide results to a few specific illustrative cases.

3.2.1. Mean field Approximation

The simplest approximation to the survival probability can be obtained without using Eqs. 13 and 15. The time rate of change of survival is simply defined as the total probability flux into absorbing states, *conditioned* on no particle having yet entered any absorbing state [25]. In our problem, the *unconditioned* instantaneous particle flux into state $L + 1$ is $J_{\text{mf}}(t) \equiv (p_L + q_L + \nu_L)\langle n_L(t) \rangle$, where $\langle n_L(t) \rangle$ is the expected occupation of state L . If we assume that the mean occupation is uncorrelated with the probability $\Sigma(t)$ of survival, $\dot{\Sigma}_{\text{mf}} \approx -J_{\text{mf}}(t)\Sigma_{\text{mf}}$. This approximation is exact when particles are always independent and is widely used. The survival probability under this mean-field assumption is thus

$$\Sigma_{\text{mf}}(t) = \exp \left[-(p_L + q_L + \nu_L) \int_0^t \langle n_L(t') \rangle dt' \right]. \quad (23)$$

The unconditioned occupation $\langle n_L(t') \rangle$ can be found using mass-action equations for the particle density at each site. The Laplace-transformed expected particle number can be written as

$$\langle \tilde{n}_L(s) \rangle = \frac{(\alpha_1 + 2\alpha_2)}{a_L s} \prod_{i=1}^L \frac{a_i}{s + b_i}, \quad (24)$$

where $a_i \equiv 2p_i + q_i + \nu_i$ and $b_i \equiv \mu_i + \nu_i + p_i - r_i$. Like Eq. 18, this result shows that the mean-field survival probability of a system injected at the first site is independent of the specific order of the rates. Moreover, upon comparing Eq. 24 to Eq. 18, we see that the mean field survival probability $\Sigma_{\text{mf}}(t) = \Sigma(t)$ is exact if $\alpha_2 = p_i = q_i = r_i = 0$.

For general rates but uniform $a_i = a$ and $b_i = b$, the general mean-field approximation for the survival probability is

$$\Sigma_{\text{mf}}(t) = \exp \left[-\frac{(\alpha_1 + 2\alpha_2)}{b} \frac{(p + q + \nu)a^{L-1}}{b^L} \left(bt - L - bt \frac{\Gamma(L, bt)}{\Gamma(L)} + \frac{\Gamma(L + 1, bt)}{\Gamma(L)} \right) \right], \quad (25)$$

which has a form analogous to Eq. 21. To explicitly see that $\Sigma_{\text{mf}}(t)$ is not exact when any $\alpha_2, p, q, r > 0$, consider the single intermediate state case $L = 1$. In this case, Eq. 17 can be solved exactly to yield explicit expressions for $S_1(t)$ and $\Sigma(t)$:

$$\Sigma(t) = e^{-\alpha_1(1-S_-)t} e^{-\alpha_2(1-S_-^2)t} \left[\frac{(S_+ - S_-)e^{\gamma t}}{(S_+ - 1)e^{\gamma t} + (1 - S_-)} \right]^{\alpha_1/r + \alpha_2\lambda/r^2} \exp \left[-\frac{\alpha_2}{r} \frac{(S_+ - 1)(1 - S_-)(e^{\gamma t} - 1)}{(S_+ - 1)e^{\gamma t} + (1 - S_-)} \right], \quad (26)$$

where

$$S_{\pm} = \frac{\lambda}{2r} \pm \frac{\lambda}{2r} \sqrt{1 - 4\mu r/\lambda^2} \quad (27)$$

and

$$\gamma = (S_+ - S_-)r = \lambda \sqrt{1 - 4\mu r/\lambda^2}. \quad (28)$$

Fig. 5 explicitly shows the difference between $\Sigma(t)$ and $\Sigma_{\text{mf}}(t)$ (Eq. 25) for various values of $\alpha_2, p, q, r > 0$. The discrepancy between the exact and mean-field results vanishes as $(\alpha_1/b)(a/b)^L/L! \gg 1$. In this limit,

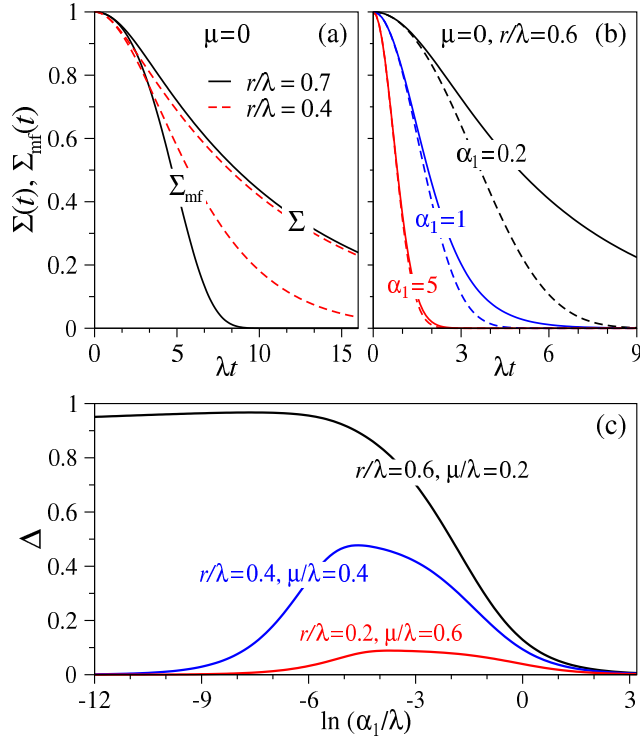


Figure 5: Comparison between exact solutions and mean-field approximations for $L = 1$. (a) $\Sigma(t)$ and $\Sigma_{\text{mf}}(t)$ for $\mu = 0$ and $r/\lambda = 0.7$ (solid) and $r/\lambda = 0.4$ (dashed). As expected, differences are larger for larger values of r/λ , where survival probability and the mean occupation $\langle n_1(t) \rangle$ share more correlations. (b) $\Sigma(t)$ (solid) and $\Sigma_{\text{mf}}(t)$ (dashed) for different values of single-particle immigration α_1 and fixed $\alpha_2 = \mu = 0, r/\lambda = 0.6$, and $(p + q + \nu)/\lambda = 0.4$. The difference is largest for smaller α_1 where immigration is rate limiting, and the first arrival at the absorbing state $k = 2$ is more likely from particles that have replicated at $k = 1$. (c) Relative errors of MFPTs $\Delta \equiv (T - T_{\text{mf}})/T$ as a function of α_1 for the combinations of $r/\lambda, \mu/\lambda$ indicated. When rates of nonlinear processes (r in this case) are large, the error is large. In the limit of vanishing r/λ , mean-field theory becomes exact and Δ vanishes.

the numbers of particles derived from independently immigrated lineages are sufficiently large such that the effects of correlations among their branching times are small. The mean-field limit can also be derived by considering the solution to S_1 in the short time limit when it deviates only slightly from unity. Linearization of Eq. 17 about $S_k = 1$ results in a set of equations whose solution also yield the mean-field result of Eq. 25.

3.2.2. Numerical results

To investigate the effects of nonlinear proliferative processes on evolution and first passage times in larger systems, we solve Eq. 17 numerically and use Eqs. 15 and 12 to find survival probabilities and MFPTs. Since Eq. 17 is nonlinear, we expect the ordering of the rates and positioning of defects along the chain to influence first passage times, in contradistinction to linear processes in which spatial ordering of rates does not play a role.

We first compare proliferative processes with an irreversible-mutation linear Moran-type process in which asymmetric differentiation occurs followed immediately by death of the parent cell. This assumption is typically used to enforce fixed population (in the absence of immigration) and in our framework corresponds to $\nu_k > 0$ and $\mu_k = p_k = q_k = r_k = 0$. This process is linear and a mean-field assumption yields exact results. A related nonlinear process can be defined by $q_k = \mu_k > 0$ (and $\nu_k = p_k = r_k = 0$). This process will give rise to identical expected populations $\langle n_k(t) \rangle$ if q_k are assigned the same values as ν_k used in the linear Moran-type process. Here, asymmetric differentiation and death are balanced such that the mean occupations are identical to those derived from the linear process $\mu_k = p_k = q_k = r_k = 0$. However, in the

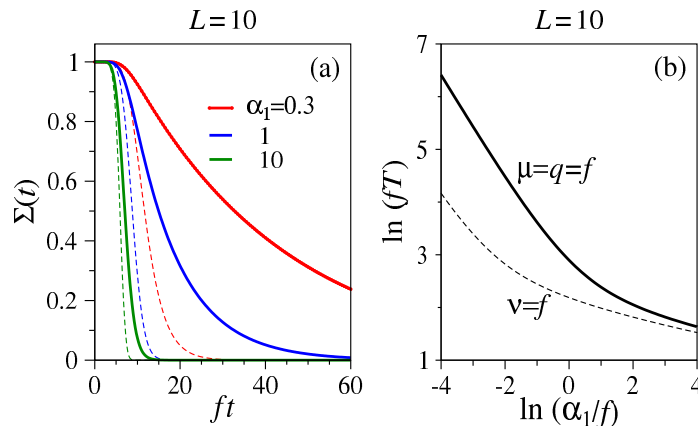


Figure 6: Comparison of two mean-field-equivalent processes $\nu = f$ and $\mu = q = f$ along a chain of length $L = 10$. (a) The dashed curves are $\Sigma(t)$ for the linear process $\nu = f$ and $\mu = p = q = r = 0$, while the thick solid curves correspond to numerical solutions of Eq. 17 for the nonlinear process $\mu = q = f$ and $\nu = p = r = 0$. Due to the independent decay processes, the MFPT of the nonlinear process is always greater than that of the linear process. (b) MFPTs as functions of $\ln(\alpha_1/f)$. Despite the mean-field equivalence, mean-field approximations to the FPTs are qualitatively inaccurate.

linear process, mutation and death of the parent particle are completely correlated, unlike in the nonlinear process ($q_k = \mu_k > 0$) in which they occur independently. The nonlinear process allows fluctuations in the total population to affect FPT statistics. In Fig. 6, $\Sigma(t)$ and the MFPTs between two processes with uniform intrinsic rate f , ($\nu = f$, $p = q = r = \mu = 0$) and ($q = \mu = f$, $\nu = p = r = 0$), are contrasted. The results in Fig. 6 can also be qualitatively understood from the likelihood of any particle at site k generating one at site $k + 1$. If $\mu = q = f > 0$, then any single cell would have a probability of only one half of generating an advancing daughter cell particle. However, in the linear Moran-type process with $\nu = f$, all particles will eventually move forward.

In the small α_1/f limit, the MFPT of the nonlinear proliferative process scales as $T \sim [\alpha_1(1 - \bar{S}_1)]^{-1}$. For $\mu = q = f$, $\bar{S}_1 = L/(L + 1)$, and $T \sim (L + 1)/\alpha_1 > T_{\text{mf}}$, where T_{mf} is the exact mean-field result for the MFPT of the linear Moran-like process, which can be found from Eq. 22 or by using Eq. 25 in Eq. 12. When α_1/f is large, the number of statistically independent particles in the system is large and the survival probability of the proliferative process will approach a common mean-field limit (Eq. 25). Thus, the relative difference between the MFPTs of the linear spontaneous mutation process and the mean-field-equivalent nonlinear process diminishes at large injection rates α_1 (and α_2). Nonetheless, cells in the proliferative process have a nonzero death rate and the MFPT is bounded above by that of the linear process. Therefore, in terms of reaching the absorbing state, we observe that the linear irreversible Moran-type process is always faster.

Next, consider another proliferative process that might be expected to yield similar FPTs as the linear Moran-like process. If cells undergo only symmetric differentiation and death with rates $p = \mu = f$ and $q = r = \nu = 0$, a parent cell can die or beget two differentiated daughters that each die at the same rate. Even though the expected populations of this process and of the irreversible Moran-type process ($\nu = f$) differ, the mean positions of the lead particle are equal (conditioned on survival). Fig. 7(a) shows the survival probabilities of the two processes for two different values of immigration. For small immigration rates α_1/f , the linear (mean-field) process reaches the absorbing state faster, while for high immigration rates, the proliferative process is faster. Fig. 7(b) plots the MFPT of the two processes as a function of injection rate. For small α_1/f , the exact MFPT T_{mf} of the linear process can again be found from the first limit in Eq. 22, while the MFPT of the nonlinear proliferative process scales as $T \approx [\alpha_1(1 - \bar{S}_1)]^{-1}$. In this case, the lineage associated with each injected cell has a possibility of becoming extinct before fixation, resulting in a MFPT diverging as $1/\alpha_1$. For $L = 10$, $\bar{S}_1 \approx 0.861$ and $T \approx (0.139\alpha_1)^{-1} > T_{\text{mf}}$. When α_1/f is large, $\Sigma(t)$ for the nonlinear proliferative process approaches the mean-field result in Eq. 25. Moreover, the

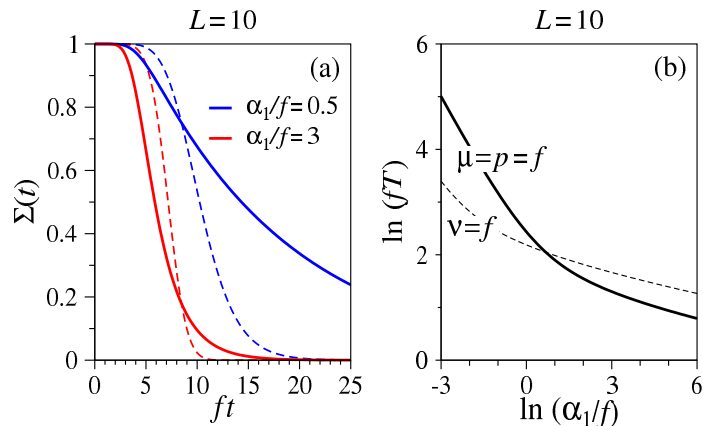


Figure 7: Comparison of two processes with similar mean lead-particle positions. (a) This dashed curves are $\Sigma(t)$ (which is equivalent to Σ_{mf}) for the linear process $\nu = f$ and $\mu = p = q = r = 0$, while the thick solid curves correspond to numerical solutions of Eqs. 17 and 15 for the nonlinear process $\mu = q = f$ and $\nu = p = r = 0$. Due to independent decay process, the MFPT of the nonlinear process is always greater than that of the linear process. (b) The MFPTs as functions of $\ln(\alpha_1/f)$ for these two processes also dramatically differ, but a cross-over occurs.

associated MFPT can be shown to be less than the MFPT for the linear process. Thus, there is a cross-over at a particular value of immigration below which the linear process becomes evolutionarily faster than the proliferative process. For large α_1 , immigration is sufficiently fast to allow overall proliferation to push lead particles to overtake those of the corresponding linear Moran-type process, leading to a smaller MFPT.

Finally, we illustrate the effects of two types of deserts (or bottlenecks) and two types of oases in an otherwise uniform evolutionary chain. Bottlenecks or deserts at site L^* may arise from an enhanced death rate μ^* , or from a suppression in ν^* , p^* , and/or q^* . A local oasis can be modeled by increased proliferation rates such as r^* or p^* . For example, Fig. 3 depicts a sequential process with an enhanced growth rate at site L^* . Fig. 8 plots the MFPT for a bottleneck (a), and an oasis (b), at different positions along the chain. For the parameters used, bottlenecks are most effective at slowing down fixation when placed near the start of the chain; conversely, an oasis is most effective at speeding up fixation when placed near the start of the chain.

The linear dependence on bottleneck position shown in Fig. 8(a) can be understood by viewing this scenario as a FPT problem in the second segment of the chain $L^* < \ell \leq L + 1$. Related sequential segmentation methods have also been used to self-consistently compute steady-state transport fluxes across excluding 1D lattices [37, 38]. Here, the bottleneck reduces the effective immigration rate into the second segment. If the bottleneck is sufficiently strong (as are the cases shown in Fig. 8(a)), immigration into the second segment is rate-limiting and since $\nu = 0$, we expect the MFPT to scale as $1/(L - L^* + 1)$.

The effect of an oasis site in the presence of an otherwise uniform process involving death and spontaneous mutation is to decrease the MFPT, as shown in Fig. 8(b). If the rates at site L^* are such that $r^* > \mu^* + \nu^*$, there can be unlimited growth and the rate of immigration into site $L^* + 1$ will exponentially increase time. Thus, an oasis near the beginning of the evolutionary chain will strongly drive immigration into the remaining segment and be more effective at reducing the MFPT to fixation compared to one that is hard to get to near the end of the chain.

An oasis with a positive net growth rate leads to an unbounded population at long times. However, our approach does not allow for interactions and constraints such as carrying capacity. Nonetheless, if the first arrival times to $L + 1$ are much smaller than the time it takes for any site to reach carrying capacity ($K \gg \exp[(r^* - \mu^*)T]$), our unlimited growth model still provides a reasonable approximation to the FPT.

In the opposite limit of small carrying capacity ($K \ll \exp[(r^* - \mu^*)T]$) another approximation to the MFPT can be obtained. We can model an oasis by assuming that in an otherwise homogeneous chain along which $p = q = r = 0$, site L^* carries a growth process with a carrying capacity K and $r^* \rightarrow r^*(1 - n_{L^*}/K)$. We also assume that $\mu^* = 0$ and that r^* is greater than all other rates in the model. Therefore, once the

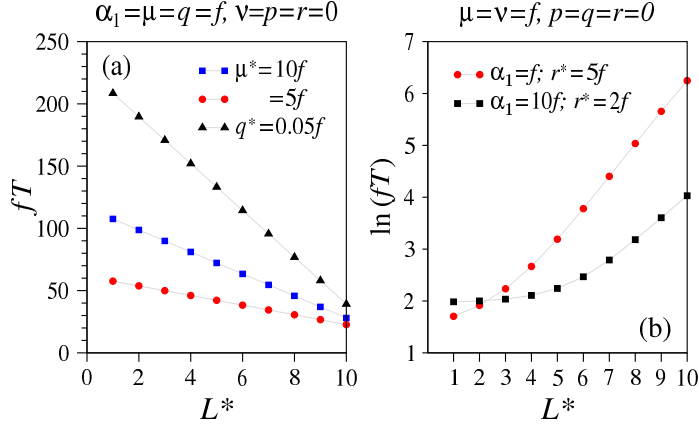


Figure 8: Spatial dependence of bottlenecks and oases. (a) Dependence of the MFPT on the position of a bottleneck. In an otherwise uniform chain with $q = \mu = f$, $\nu = p = r = 0$, cells at site L^* die with increased rates $\mu_{L^*} \equiv \mu^* = 5f$ (red circles) and $\mu^* = 10f$ (blue squares). Alternatively, this bottleneck site may have a diminished asymmetric division rate $q_{L^*} \equiv q^* = 0.05f$ (black triangles). (b) The dependence of the MFPT on the position of an oasis at a site with no death ($\mu_{L^*} = 0$), enhanced growth rates $r_{L^*} \equiv r^* = 2f, 5f$, and corresponding immigration rates $\alpha_1 = f$ and $\alpha_1 = 10f$, respectively. In the rest of the chain, there are no proliferative processes ($p = q = r = 0$) and cells both spontaneously mutate and die with rate $\nu = \mu = f$.

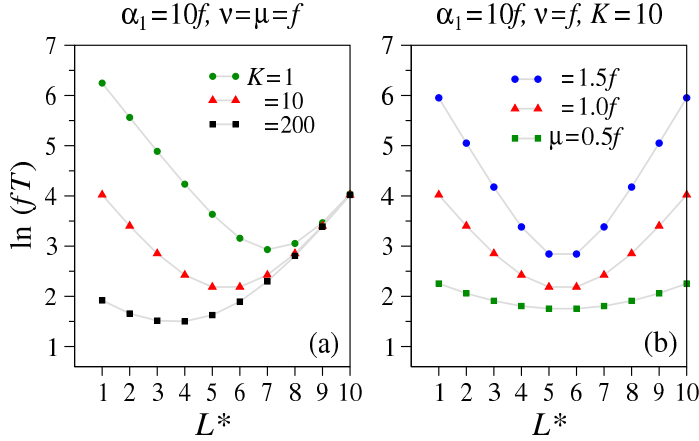


Figure 9: MFPT in the presence of an oasis with large growth rate $r^* \rightarrow \infty$ but a finite carrying capacity K . (a) $\ln fT$ for various carrying capacities K at fixed immigration rate $\alpha_1 = 10f$ and spontaneous mutation and death rate $\nu = \mu = f$. (b) When $\alpha_1 = K\nu = 10f$, both effective immigration rates are equal and the MFPT-minimizing position $L^* \approx L/2$ (Eq. 30).

first particle arrives at site L^* , its population quickly rises to a level $\sim K$. These cells then feed into site $L^* + 1$ through mutational processes described by ν, p , or q . By considering two linear processes joined by an oasis at site L^* , the MFPT to state $L + 1$ can be approximated as the mean time to reach L^* plus the time to reach state $L + 1$ given an effective immigration rate $K\nu$ into site $L^* + 1$. Not only does the MFPT depend on the spatial structure of the inhomogeneity, but in many cases, there will be an optimal placement of an oasis which most effectively reduces the overall MFPT. Such an optimal placement can be explicitly seen by considering Eq. 22 in the small immigration limit:

$$\begin{aligned}
 T(L, L^*) &\approx T(L^* - 1) + T(L - L^*) \\
 &\approx \frac{1}{\Omega\lambda} + \frac{1}{\Omega^*\lambda} + \frac{L}{\lambda},
 \end{aligned} \tag{29}$$

where $\Omega \equiv (\alpha_1/\lambda)(\nu/\lambda)^{L^*-1}$ and $\Omega^* \equiv (K\nu/\lambda)(\nu/\lambda)^{L-L^*}$. This approximation clearly shows a position-dependent MFPT provided $\nu/\lambda < 1$ ($\mu > 0$). The position L_{\min}^* which yields the smallest MFPT in the $\Omega L^*, \Omega^*(L - L^*) \ll 1$ limit can be approximated by solving $\partial T(L, L^*)/\partial L^* = 0$:

$$L_{\min}^* \approx \frac{\ln\left(\frac{\alpha_1}{K\nu}\right)}{2 \ln\left(\frac{\Delta}{\nu}\right)} + \frac{L+1}{2}, \quad (30)$$

which shows that when $K\nu \approx \alpha_1$, the oasis lowers the MFPT the most when placed near the midpoint of the chain. Eq. 30 provides good estimates of the optimal oasis position L_{\min}^* and its dependences on rates.

In Fig. 9(a) we use Eqs. 15 and 12 to compute the MFPT of a two-segment chain. For the segment before the oasis, we use $T(L^* - 1) = \int_0^\infty \Sigma(t; \alpha_1 = f, \mu = \nu = f, L^* - 1) dt$, while for the second segment, $T(L - L^*) = \int_0^\infty \Sigma(t; \alpha_1 \equiv K\nu, \mu = \nu = f, L - L^*) dt$. Evaluating the total MFPT $T(L^* - 1) + T(L - L^*)$ clearly shows that the most effective positioning of an oasis is such that the segment with rate-limiting immigration is shortest. Since changes in μ only affect L_{\min}^* logarithmically, small changes in the death rate do not affect the optimal oasis position. However, when μ increases, as shown in Fig. 9(b), the MFPTs across each segment increases exponentially with its length, increasing the sensitivity of the overall MFPT to L^* .

4. Discussion & Conclusions

We have formulated an efficient way to analyze FPTs on a network containing multiple, mutating, and proliferating particles. Our model allows one to naturally study stochastic evolutionary processes and explicitly include cell fate decisions, fluctuations in total number, and immigration. A number of asymptotic limits are explored and comparisons with mean-field calculations of survival probabilities performed. Kinetic Monte Carlo simulations were also performed and checked against our results. Our main findings illustrate the importance of specific cellular transitions and how mean-field assumptions can be misleading when used to compute first arrival times. Even though expected particle numbers of a noninteracting particle system can typically be found exactly using mean-field approximations, our results explicitly show how survival probabilities and first passage time statistics cannot be treated using simple mean-field approximations if particles can proliferate. These discrepancies are prominent in conditions of low populations, as encountered in stochastic tunneling.

Furthermore, proliferative processes, including symmetric and asymmetric cell differentiation, render FPTs dependent on the order of the transition rates along a sequential evolutionary chain. For many scenarios, we find bottlenecks are most effective at increasing the MFPT when placed at the beginning of an evolutionary chain, while an unlimited oasis reduces the MFPT most effectively at the beginning of the chain. If the growth rate of an oasis site is faster than any other time scale, the mean times to the terminal state can be approximated by the mean time for the first cell to arrive at the oasis, plus the time for the progeny of any cell arising from an oasis to arrive at the terminal site. In the presence of regulating interactions that generate *e.g.*, a carrying capacity K , we find intermediate oasis positions that optimally reduce the MFPT to the final $L + 1$ -state. This optimal position is qualitatively determined by the ratio of the effective immigration rates into each of the segments and deviates from the halfway point by the log of the ratio of immigration rates, with the shorter segment associated with the smaller effective immigration rate.

Collectively, our results suggest that fixation times across a number of biological systems may be sensitive to the precise transitions allowed. Examples include stem cell differentiation [2] and mutation [29], where each differentiation or mutational state is represented by distinct nodes. Our approach is also particularly appropriate for modeling progression and drug resistance in cancer. Since mutated or precancerous cells may likely have only a small fitness advantage [18], the numbers of cells in these states may be small, and the effects of proliferative nonlinearity may be important. In such cases, cell states that are drug resistant will do the most harm when occurring at the beginning, or in the interior of the mutational sequence, depending on, respectively, whether a carrying capacity arises or not. We have investigated only simple, irreversible transitions along a 1D sequential chain. Extensions to more complex networks and

nonexponentially distributed processes (such as cell-cycle timing) can be readily investigated by numerically solving Eqs. 9 and 11. More complex distributions of different transition rates can also be easily treated numerically.

5. Acknowledgements

TC was supported by the NSF through grant DMS-1021818, the Army Research Office through grant 58386MA, and the DoD through grant W911NF-13-1-0117. YW was supported through the Cross-disciplinary Scholars in Science and Technology (CSST) program at UCLA. The authors also wish to acknowledge the support of the KITP at UCSB through NSF PHY11-25915.

References

- [1] A. Marciniak-Czochra, T. Stiehl, A. D. Ho, W. Jager, W. Wagner, Modeling of asymmetric cell division in hematopoietic stem cells-regulation of self-renewal is essential for efficient repopulation, *Stem Cells and Development* 18 (2009) 377–385.
- [2] A. Roshan, P. H. Jones, C. D. Greenman, Exact, time-independent estimation of clone size distributions in normal and mutated cells, *J. Roy. Soc. Interface* 11 (2014) 20140654.
- [3] C. D. Sherman, C. J. Portier, Stochastic simulation of a multistage model of carcinogenesis, *Mathematical Biosciences* 134 (1996) 35–50.
- [4] C. J. Portier, C. D. Sherman, A. Kopp-Schneider, Multistage, stochastic models of the cancer process: A general theory for calculating tumor incidence, *Stochastic Environmental Research and Risk Assessment* 14 (2000) 173–179.
- [5] A. Bellacosa, Genetic hits and mutation rate in colorectal tumorigenesis: versatility of Knudson’s theory and implications for cancer prevention, *Genes, Chromosomes & Cancer* 38 (2003) 382–388.
- [6] S. L. Spencer, R. A. Gerety, K. J. Pienta, S. Forrest, Modeling somatic evolution in tumorigenesis, *PLoS Computational Biology* 2 (2006) e108.
- [7] C. S.-O. Attolini, Y.-K. Cheng, R. Beroukhi, G. Getzand, O. Abdel-Wahab, R. L. Levine, I. K. Mellinohoff, F. Michor, A mathematical framework to determine the temporal sequence of somatic genetic events in cancer, *Proceedings of the National Academy of Sciences USA* 107 (2010) 17604–17609.
- [8] T. Antal, P. L. Krapivsky, Exact solution of a two-type branching process: Models of tumor progression, *Journal of Statistical Mechanics: Theory and Experiment* 2011 (2011) P08018.
- [9] S. A. Frank, Age-specific incidence of inherited versus sporadic cancers: a test of the multistage theory of carcinogenesis, *Proc. Natl. Acad. Sci. USA* 102 (2005) 1071–1075.
- [10] L. J. S. Allen, *An Introduction to Stochastic Processes with Applications to Biology*, Pearson Prentice Hall, Upper Saddle NJ, 2003.
- [11] T. Antal, P. L. Krapivsky, Exact solution of a two-type branching process: Clone size distribution in cell division kinetics, *Journal of Statistical Mechanics* (2010) P07028.
- [12] P. Armitage, R. Doll, The age distribution of cancer and a multi-stage theory of carcinogenesis, *Int. J. Epidemiol.* 33 (2004) 1174–1179.
- [13] S. H. Moolgavkar, A. G. Knudsen, Mutation and cancer: a model for human carcinogenesis, *J. Natl. Cancer Inst.* 66 (1981) 1037–1052.
- [14] A. G. Knudsen, Mutation and Cancer: Statistical Study of Retinoblastoma, *Proc. Natl. Acad. Sci. USA* 68 (1971) 820–823.
- [15] P. H. Fitzgerald, J. Stewart, R. D. Suckling, Retinoblastoma mutation rate in New Zealand and support for the two-hit model, *Human Genetics* 64 (1983) 128–130.
- [16] D. L. Floyd, S. C. harris, A. M. van Oijen, Analysis of kinetic intermediates in single-particle dwell-time distributions, *Biophys. J.* 99 (2010) 360–366.
- [17] R. J. Rieker, J. Hoegel, M. A. Kern, C. Steger, S. Aulmann, G. Mechttersheimer, P. Schirmacher, H. Blaeker, A mathematical approach predicting the number of events in different tumors, *Pathol. Oncol. Res.* 14 (2000) 199–204.
- [18] N. Beerenwinkel, T. Antal, D. Dingli, A. Traulsen, K. W. Kinzler, V. E. Velculescu, B. Vogelstein, M. A. Nowak, Genetic progression and the waiting time to cancer, *PLoS Comput Biol* 3 (2007) e225.
- [19] S. Hwang, D.-S. Lee, B. Kahng, First passage time for random walks in heterogeneous networks, *Phys. Rev. Lett.* 109 (2012) 088701.
- [20] E. Agliari, Exact mean first-passage time on the T-graph, *Phys. Rev. E* 77 (2008) 011128.
- [21] K. Lindenberg, V. Seshadri, K. E. Shuler, G. H. Weiss, Lattice random walks for sets of random walkers: First passage times, *J. Stat. Phys.* 23 (1980) 11–25.
- [22] X. Li, A. B. Kolomeisky, A. Valleriani, Pathway structure determination in complex stochastic networks with non-exponential dwell times, *J. Chem. Phys.* 140 (2014) 184102.
- [23] G. Bal, T. Chou, On the reconstruction of diffusions using a single first-exit time distribution, *Inverse Problems* 20 (2003) 1053–1065.
- [24] P.-W. Fok, T. Chou, Reconstruction of bond energy profiles from multiple first passage time distributions, *Proc. Roy. Soc. A* 466 (2010) 3479–3499.
- [25] T. Chou, M. R. D’Orsogna, *First Passage Problems in Biology*, in *First-Passage Phenomena and Their Applications*, World Scientific, 2014.

- [26] Y. Isawa, F. Michor, M. Nowak, Stochastic tunnels in evolutionary dynamics, *Genetics* 166 (2004) 1571–1579.
- [27] D. M. Weinreich, L. Chao, Rapid evolutionary escape, *Theoretical Population Biology* 75 (2009) 286–300.
- [28] D. B. Weissman, M. Desai, D. S. Fisher, M. W. Feldman, The rate at which asexual populations cross fitness valleys, *Theoretical Population Biology* 75 (2009) 286–300.
- [29] P. T. McHale, A. Lander, The Protective Role of Symmetric Stem Cell Division on the Accumulation of Heritable Damage, *PLoS Comp. Biol.* 10 (2014) e1003802.
- [30] K. B. Athreya, P. E. Ney, *Branching Processes*, Springer, New York, 1972.
- [31] P. Fok, T. Chou, Identifiability of age-dependent branching processes from extinction probabilities and number distributions, *Journal of Statistical Physics* 152 (2013) 1–18.
- [32] P. Jagers, Age-dependent branching processes allowing immigration, *Theory of Probability and its Applications* 13 (1968) 225–236.
- [33] R. Shonkwiler, On age-dependent branching processes with immigration, *Comp. & Maths. with Appls.* 6 (1980) 289–296.
- [34] S. Redner, *A guide to first-passage processes*, Cambridge University Press, 2001.
- [35] B. H. Shargel, M. R. D’Orsogna, T. Chou, Arrival times in a zero-range process with injection and decay, *J. Phys. A* 43 (2010) 305003.
- [36] C. M. Bender, S. A. Orszag, *Advanced Mathematical Methods for Scientists and Engineers: Asymptotic Methods and Perturbation Theory*, Springer-Verlag, New York, 1999.
- [37] A. B. Kolomeisky, Asymmetric simple exclusion model with local inhomogeneity, *J. Phys. A: Math. Gen.* 31 (1998) 1153–1164.
- [38] T. Chou, G. Lakatos, Clustered bottlenecks in mRNA translation and protein synthesis, *Phys. Rev. Lett.* 93 (2004) 198101.